Development of gasoline-ethanol blends laminar flame speed correlations at full-load Si engine conditions via 1D simulations

Cite as: AIP Conference Proceedings **2191**, 020063 (2019); https://doi.org/10.1063/1.5138796
Published Online: 17 December 2019

Marco Del Pecchia, Valentina Pessina, Clara Iacovano, and Giuseppe Cantore

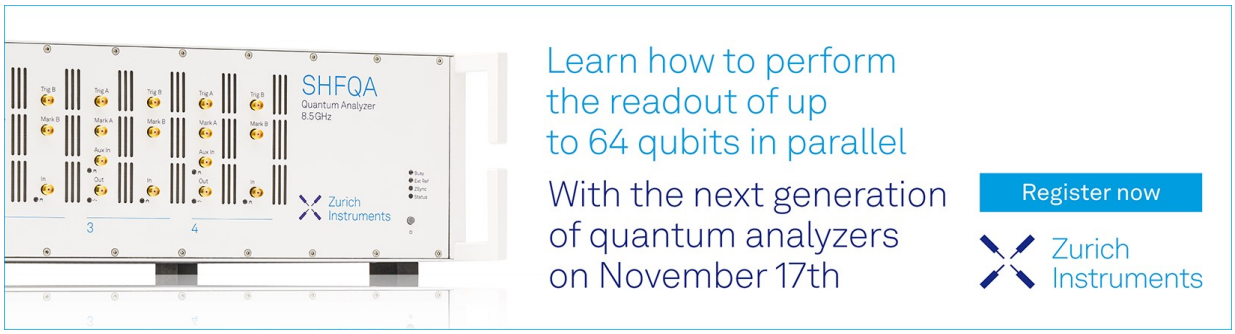

Development of Gasoline-Ethanol Blends Laminar Flame Speed Correlations at Full-Load SI Engine Conditions via 1D simulations

Marco Del Pecchia [1, a)], Valentina Pessina [1], Clara Iacovano [1], Giuseppe Cantore [1]

[1] Department of Engineering "Enzo Ferrari", University of Modena and Reggio Emilia, Via Vivarelli 10, Modena 41125, Italy

[a)]Corresponding author: marco.delpecchia@unimore.it

Abstract. Nowadays, most of the engineering development in the field of Spark-Ignited (SI) Internal Combustion Engines (ICEs) is supported by 3D-CFD simulations relying on flamelet combustion models. Such kind of models require laminar flame speed as an input to be specified by the user. While several laminar flame speed correlations are available in literature, for gasoline and pure ethanol at ambient conditions, there is a lack of correlations describing laminar flame speed of gasoline-ethanol blends, for different ethanol volume content, at conditions deemed to be representative of engine-like conditions. Toluene Reference Fuel surrogates with addition of ethanol (ETRF), suitable for representing gasoline-ethanol blends up to 85% vol. ethanol content are formulated. Thanks to these surrogates, 1D premixed laminar flame speed calculations are performed at selected engine-relevant conditions for a E5, E20 and E85 fuels. As a final outcome, three different laminar flame speed correlations based on the chemistry-based calculations are derived for E5, E20 and E85 gasoline-ethanol fuel blends focusing on typical full-load engine conditions. Such kind of correlations can be easily implemented in any 3D-CFD code to provide a chemistry-grounded estimation of laminar flame speed during combustion calculations. Such correlations are of practical use, since they might help in developing the next generation of bio-fuels powered internal combustion engines.

INTRODUCTION

As reported in the Official Journal of the European Union (EU) [1], the threat of the climate change and global warming have pushed the EU to set very challenging targets in order to firmly decrease the anthropogenic greenhouse gas (GHG) emissions. According to a proposal for the regulation by the European parliament and council [2], the road transport was responsible for 22% of EU GHG emissions in 2015. For this reason, a Renewable Energy Directive (REDII) [3] introduced a binding obligation according to which 10% of the energy used in traffic must be bio-based by 2020. The same directive imposes to fuel suppliers that 6.8% market share by 2030 of low-emissions and renewable fuels, including advanced bio-fuels. Based on the scenario previously described, bio-fuels have increasingly gained the attention of researchers and developers in the automotive industry as a feasible solution to move towards cleaner powertrains, in compliance with the EU regulations. Being a renewable source of energy with lower production costs compared to other alcohols, such as n-butanol or methanol, ethanol has become the dominant bio-fuel used in current production engines [4,5]. For this reason, several experimental studies investigated the effect of pure bio-alcohols fueling on combustion characteristics in modern direct-injection spark-ignition engines (DISI). Among those studies, in [6] Irimescu et al. compared the effect of stoichiometric butanol and ethanol fueling at WOT on combustion behavior and emissions performance, compared with standard gasoline fueling, in an optically accessible DISI research unit. In order to investigate the sensitivity of the performance with different strategies of these fuels, three different start of injections (SOI) were selected. In general, ethanol exhibited advantages in terms of HC and CO emissions. Nevertheless, a non-negligible decrease of performance was found for deviations from the optimum injection phasing. As an overall conclusion, the study showed that control strategies need to be adapted when using pure ethanol fueling. Moreover, several studies [7, 8, 9] reported the impossibility of performing pure ethanol fueling strategy with standard engine hardware because of the damages caused by the its intrinsic high corrosiveness to the components of the injection systems. Contrarily, other studies report that minor hardware modifications and adjustments to the electronic control unit (ECU) are needed up to 30% ethanol content by volume [10,11]. Therefore, many researchers focused the attention on gasoline-ethanol blends as a feasible

74th ATI National Congress
AIP Conf. Proc. 2191, 020063-1–020063-12; https://doi.org/10.1063/1.5138796
Published by AIP Publishing. 978-0-7354-1938-4/$30.00

compromise to meet the upcoming regulations retaining the overall architecture of modern DISI units. Several experimental studies were carried out on standard SI units, with different architectures and injection systems, powered by gasoline-ethanol blends with different blending ratios and tested on different operating points (OP). As a general trend, each experimental dataset confirms the benefits in terms of carbon monoxide (CO) and unburnt hydrocarbons (UHC) emissions reduction increasing the ethanol content in the blend [9,12,13,14,15,16,17,18]. The impact of gasoline-ethanol fueling on nitrogen oxides emissions is still a widely debated topic in the researchers' community since no clear trends emerge from the literature. While in [13,18] increasing emissions were registered with an increasing ethanol content, opposite results were found in [14,16]. The opposed trends shown by different experimental campaigns can be explained by the high sensitivity exhibited by nitrogen oxides to the specific engine OP and ethanol content, as shown in [12,15]. With respect to soot emissions, several studies clearly demonstrated that soot mass can be strongly decreased if gasoline is blended with ethanol and that soot mass reduction is proportional to the ethanol content [19,20,21,22]. While gasoline-ethanol fuel blends constitute a promising solution to further improve the environmental impact of the GDI technology, it is also clear that further efforts are mandatory in order to enhance the performance of the combustion system over the complete range of OPs covered by the engine. Further optimizations of the control strategy to decrease the engine-out emissions retaining the same power output are therefore required. An unprecedented insight to understand the key reasons behind the overall behavior of the engine depicted by the experiments can be provided by 3D CFD numerical simulations. When simulating turbulent combustion processes in SI units, flamelet combustion models are widely adopted in the scientific community: within such family, the ECFM-3Z [23] and the G- equation [24] are among the most commonly adopted. Despite the description of the combustion process development is based on different approaches, both models require the laminar flame speed s_L as an input in order to properly estimate the turbulent combustion rate. Most of the CFD codes estimate s_L based on correlations derived via fitting approaches of experimental campaigns carried out over a wide range of conditions, such as Metghalchi and Keck's [25] or Gülder's formulation [26] for Isooctane. Being s_L an intrinsic characteristic of the fuel mixture, it is straightforward that specific correlations are needed to describe the propagating characteristics of a given fuel at specific thermodynamic conditions, identified by the ambient pressure (p), the unburnt mixture temperature (T_u), the equivalence ratio (Φ) and the dilution rate (expressed as the residuals mass fraction Y_{res}). Gülder in [27] and Broustail et al. in [28], derived laminar flame speed correlations for isooctane-ethanol blends based on atmospheric pressure experiments. Such kind of correlations are useful to evaluate the impact of ethanol content on flame propagation but are not suitable to quantitatively predict laminar flame speed at engine-relevant conditions. In fact, a non-negligible error is introduced extrapolating beyond the correlations' validity range. As a result, most of the correlations available in literature are of very limited practical use to reliably predict laminar flame speed of gasoline-ethanol blends, at thermodynamic and mixture quality states of interest for SI engines, especially in their full-load operating range. In the present work, Toluene Reference Fuel surrogates with addition of ethanol (ETRF) are formulated with a methodology developed by the authors. The former aims at formulating ETRF surrogates able to represent the auto-ignition characteristics, the flame propagation characteristics and the main chemico-physical properties of the most widespread gasoline-ethanol blends. In the following paragraph, an innovative methodology to formulate laminar flame speed correlations is briefly recalled by the authors' previous works on the topic [29, 30] and results from chemistry-based 1D premixed flamed simulations are presented for three selected blends (E5, E20 and E85).

FORMULATION OF GASOLINE-ETHANOL SURROGATES

Detailed chemical kinetics calculations rely on the definition of a proper fuel model to give a quantitative description of a specific fuel characteristic (e.g. ignition delay, laminar flame speed, sooting tendency, etc.) at given thermodynamic and mixture quality conditions. A fuel model is defined when a fuel surrogate, suitable for mimicking a set of specific chemical and physical fuel properties relevant for combustion simulations (e.g. H/C ratio, O/C ratio, Density, LHV, RON, MON, etc.), and a chemical kinetics mechanism, to predict the main oxidation pathways by which reactants are converted into combustion products, are properly chosen. In order to formulate a surrogate, the chemical and physical properties of the targeted fuel are needed [31]. When referring to a generic gasoline-ethanol blend, the capital letter "E" followed by an integer number indicates the ethanol content by volume [32]. Considered that ethanol content by volume is uniquely identified once the targeted gasoline-ethanol blend is chosen (e.g. E5, E10, E20, E30, E85, etc.), a suitable fuel surrogate is needed to model the gasoline content. Several studies have shown that mixtures of isooctane, n-heptane and toluene, known as Toluene Reference Fuels (TRFs), can predict with a high degree of accuracy the auto-ignition characteristics of commercial gasolines [33, 34, 35 36]. In previous works [29, 30] by the authors, two different fuel surrogates, to be used with different chemical kinetics

mechanisms, were used to perform laminar flame speed calculations. The aforementioned TRF surrogates were proposed in literature as promising candidates to mimic the auto-ignition and flame propagation characteristics of a $RON87$ [33] and a $RON95$ [31, 38] gasoline respectively. As reported in [41], refined gasoline fuels are complex mixtures of hydrocarbons that often vary with location and time. Therefore, a statistically-relevant "average gasoline", denoted $ULG95$ [31], is used as a basis for the formulation of the gasoline-ethanol blends. All the relevant ULG95 gasoline properties targeted in the present work, are from known on identified by the superscript "gas". With particular reference to the present work, providing a set of laminar flame speed correlations for three different blending ratios of the same base blend implies that also the main chemical and physical properties of the targeted blends are accurately represented by the formulated surrogates. For this reason, a new methodology, based on the work by Pera et al. [31], is here used for the purpose of formulating suitable surrogates to represent the main chemico-physical properties, the auto-ignition propensity and freely propagating flame characteristics of the targeted fuel. Due to the fact that no data on $ULG95$ laminar flame speed are available in literature, the laminar flame speed dataset provided by Jerzembeck et al. in [39] for a generic commercial gasoline, at 373 K and pressure conditions representative of an engine-like environment, are considered. Among the different chemico-physical properties, H/C ratio plays a fundamental role in defining other properties such as lower heating value (LHV), density, stoichiometric air-to-fuel ratio (AFR) and boiling point [31]. Undoubtedly, fuel's AFR must be matched with high accuracy because the laminar flame speed correlation will rely on equivalence ratio Φ, as an input parameter, to estimate s_L. Finally, in order to have a surrogate which is representative of the auto-ignition characteristics, Research Octane Number (RON) is selected as a further constraint. The methodology proposed by Pera et al. [31], is suitable for generating a surrogate matching many different properties (e.g. H/C ratio, O/C ratio, RON, MON) solving a simple linear system. Unfortunately, no information on the surrogate's capability to represent the laminar flame propagating characteristics of the fuel are provided. A new methodology to take into account the influence of the surrogate's composition on the flame propagation characteristics is hereafter presented. In [40] Sileghem et al. demonstrated that a TRF-based mixing rule can be used to predict commercial gasoline's laminar flame speed over a given temperature range. In [42] the same authors investigated the capability of simple mixing rules to predict gasoline-ethanol blends' laminar flame speed. The results proved that simple mixing rules that consider only the change in the composition are accurate enough to predict s_L of ethanol/hydrocarbon blends. In literature a wide variety of mixing rules is available but for the present study only Le Chatelier's [43] mixing rule is considered. The proposed formula was successfully used by Benedetto et al. [43] to predict hydrogen-methane premixed flames s_L up to 10 bar and 400 K. Based on Eq.1, reporting Le Chatelier's mixing rule, it is possible to notice that the final mixture's s_L is estimated based on the mole fraction and laminar flame speed of the pure components.

$$s_{L,blend}(\Phi) = \frac{1}{\sum_{i=1}^{n} \frac{x_i}{s_{L,i}(\Phi)}} \tag{1}$$

where x_i and $s_{L,i}$ are, respectively, the mole fraction and the laminar flame speed of the i^{th} component and n is the number of components used in the blend. Based on the same rationale, a mathematical formulation is needed to estimate the auto-ignition characteristics of a fuel blend. While several studies suggested complex mathematical formulation [35, 44], the averaging of compound values weighted by molar fractions suggested in [31] is used in the present study. Despite its simple form, presented in Eq.2, this approach allows to retain the same degree of accuracy of the formulations proposed in [37, 48] and it is able to replicate the non-linear blending effect of certain components (e.g. n-heptane and toluene).

$$RON_{blend} = \sum_{i=1}^{n} x_i RON_i \tag{2}$$

where x_i and RON_i are, respectively, the mole fraction and the research octane number of the i^{th} component and n is the number of components used in the blend. As previously highlighted, it is mandatory to properly represent the fuel's H/C ratio, whose estimation can be done using Eq.3:

$$H/C_{blend} = \frac{\sum_{i=1}^{n} x_i H_i}{\sum_{i=1}^{n} x_i C_i} \tag{3}$$

where x_i, H_i, C_i are the mole fraction and the research octane number of the i^{th} component, the number of hydrogen and carbon atoms in species i and n is the number of components used in the blend. It is important to notice that total molar fraction equal to unity constraint, expressed by Eq. 4, must be introduced.

$$\sum_{i=1}^{n} x_i = 1 \tag{4}$$

Since ULG95 was chosen as the reference real fuel to be targeted, the left hand side terms in Eq.2-3, can be replaced with ULG95's research octane number (RON_{gas}) and H/C ratio (H/C_{gas}) respectively. These numerical values are explicitly reported in Table 1 for ULG95. In the same manner, a numerical reference value for the generic $s_{L,blend}(\Phi)$ term must be found. Since laminar flame speed measurements are not available, at engine-relevant conditions, for ULG95 gasoline, the laminar flame speed dataset for a commercial gasoline reported in [39] by Jerzembeck, et al. [39] is targeted. The former reports laminar flame speed values for a single temperature level ($373\ K$) and different pressure levels ($10\ bar - 25\ bar$) in the equivalence ratio range $\Phi = 0.7 \div 1.2$.
Once a specific pressure and equivalence ratio values are chosen, the term $s_{L,blend}(\Phi)$ can be substituted with a specific experimental laminar flame speed value $s^*_{L,gas}$ from [39]. The objective of the proposed methodology is the formulation of a suitable isooctane/n-heptane/toluene-based surrogate matching the previously highlighted properties This leads to an overdetermined system of four equations in three unknowns ($x_{iso}, x_{nhept}, x_{tol}$). Having identified the target fuel properties (H/C_{gas}, RON_{gas}, $s_{L,gas}$) and suitable relationships to estimate the blend properties the linear system of four equations, reported in Eq.5, is obtained:

$$\begin{cases} x_{iso}+x_{nhept}+x_{tol} = 1 \\ \dfrac{x_{iso}H_{iso}+x_{nhept}H_{nhept}+x_{tol}H_{tol}}{x_{iso}C_{iso}+x_{nhept}C_{nhept}+x_{tol}C_{tol}} = H/C_{gas} \\ x_{iso}RON_{iso}+x_{nhept}RON_{nhept}+x_{tol}RON_{tol} = RON_{gas} \\ \dfrac{1}{\dfrac{x_{iso}}{s_{L,iso}}+\dfrac{x_{nhept}}{s_{L,nhept}}+\dfrac{x_{tol}}{s_{L,tol}}} = s^*_{L,gas} \end{cases} \tag{5}$$

where $s^*_{L,iso}$, $s^*_{L,nhept}$ and $s^*_{L,tol}$ are the laminar flame speed valued for isooctane, n-heptane and toluene, respectively, at the thermodynamic and mixture quality conditions ($p^*, T^*_u, \Phi^*, EGR^*$) for which $s^*_{L,gas}$ was measured in [39]. The laminar flame speed values for the pure components is estimated via 1D laminar flame speed simulations, using DARS v4.30 chemistry solver licensed by SIEMENS PLM. The chemical kinetics mechanisms used to compute such kind of calculations and the post-processing technique used to obtained the final s_L values will be presented in the next section.
Despite its form, the linear system can still be solved using a least squares approach. A comparison between ULG95 gasoline's properties [31, 38] and the ones of the TRF surrogate obtained with the presented methodology is summarized in Table 1.

	ACA [-]	AHA [-]	AOA [-]	RON [-]*	MON [-]	AKI [-]	Sensitivity [-]	H/C* [-]	O/C [-]	α_s [-]	LHV [MJ/kg]	ρ at 298 K [kg/m^3]
ULG95	6.760	12.480	0.080	95	85	90	10	1.801	0.011	14.254	42.801	749.00
TRF	7.409	13.207	0.000	95.12	87.67	91.39	7.45	1.782	0.000	14.416	42.714	752.57

TABLE 1. Comparison between targeted gasoline and formulated surrogate's properties. *Targeted Properties

In Table 1, ACA, AHA and AOA are the average number of carbon, hydrogen and oxygen atoms constituting the surrogate's average formula. The so-called Anti-Knock Index (AKI), which is defined as the arithmetic average of RON and MON, is also reported in Table 1, to further compare the surrogate's and the reference fuel's properties. It is important to notice that only the marked ("$*$") quantities, in Table 3, were effectively targeted. In order to further assess the capability of the present surrogate to reproduce the flame propagation characteristics of a commercial gasoline, 1D laminar flame speed calculations were carried out with the methodology presented by the authors in [30] on a selection of conditions from the targeted Jerzembeck's s_L dataset [39]. Two different chemical kinetics mechanisms [39, 49] and the proposed TRF surrogate were used. A comparison between the experiments, the s_L predicted by Le Chatelier's mixing rule and the calculated s_L is reported in Fig. 1:

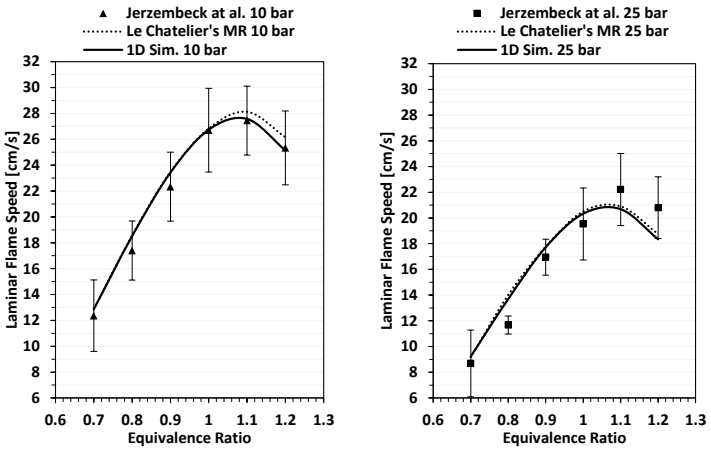

FIGURE 1. s_L at 373 K and two different pressure levels: 10 bar and 25 bar. Experiments with error bars (dots), Le Chatelier's mixing rule's predictions (dotted line) and chemistry-based calculated data (solid line) with the proposed surrogate are reported.

Therefore, it is possible to conclude that the calculated surrogate $\bar{x}^f = \left|x^f_{iso} = 40.94\%mol, x^f_{nhept} = 13.91\%mol, x^f_{tol} = 45.15\%mol\right|$ is actually able to match the chemico-physical properties, the auto-ignition propensity and the flame propagation characteristics of ULG95 gasoline. At this point, a family of gasoline-ethanol fuel surrogates can be generated since ethanol content in volume is imposed, by definition, and TRF components are scaled accordingly. The compositions of the resulting gasoline-ethanol blends' surrogates are reported in Table 2 while their corresponding properties are reported in Table 3.

[%mol]	E5	E20	E85
Isooctane	36.49	25.92	2.90
n-Heptane	12.40	8.81	0.98
Toluene	40.24	28.59	3.20
Ethanol	10.87	36.68	92.92

TABLE 2. Composition of the formulated Gasoline-Ethanol blend surrogates

	Eth [%vol]	ACA [-]	AHA [-]	AOA [-]	RON* [-]	MON [-]	H/C* [-]	O/C [-]	α_s [-]	LHV [MJ/kg]	ρ at 298 K [kg/m^3]	T_b [K]
E5	5	6.822	12.424	0.109	96.52	87.92	1.821	0.016	14.133	40.984	754.19	374.50
E20	20	5.426	10.564	0.367	99.84	88.52	1.947	0.068	13.289	36.878	759.06	367.85
E85	85	2.383	6.510	0.929	107.09	89.83	2.732	0.390	9.755	27.927	780.14	353.35

TABLE 3. Properties of the formulated Gasoline-Ethanol blend surrogates

In Table 3, T_b is the molar averaged boiling point of the mixture, which gives the most accurate reflection of the distillation characteristics of the blend.

LAMINAR FLAME SPEED CORRELATIONS AND RESULTS

In the previous paragraph, a family of suitable gasoline-ethanol blends surrogates were formulated. In this section, the validation of the fuel model (mechanisms and surrogates) on a non-representative engine test condition and a brief summary of the laminar flame speed methodology proposed by the authors in [29, 30] is addressed. When it comes to s_L fuel model validation, a general lack of laminar flame speed experimental data at engine-relevant condition is found. Despite being of little interest for the purpose of the present study, the approach used by the authors for laminar flame speed modelling is validated against isooctane-ethanol laminar flame speed experimental data at ambient conditions and 358 K [40]. Basically, the laminar flame speed calculations are carried out with two [37, 45], extensively validated [29, 30], mechanisms using the very same isooctane-ethanol blends used in the experiments, with varying ethanol content. It must be noted that the final s_L estimation is calculated via a linear averaging of the two datasets. This procedure is used to account for the possible mechanism-dependent deviations introduced while relying on a single mechanism, which is usually due to possible differences in the main oxidation

pathways of the C1-C4 hydrocarbon classes among different mechanisms. Furthermore, this particular procedure was previously validated by the authors in [29, 30] A comparison between the experimental and computed values of s_L is reported in Fig. 2. The results obtained with the fuel model are in fairly good agreement with the experimental results, considering that the error range is estimated to be $\pm 1\ cm/s$ for $\Phi < 1.3$. The higher deviations obtained for very rich mixtures ($\Phi \geq 1.3$) are considered acceptable, since a higher experimental error is reported to be present in the experiments for ≥ 1.3 due to the arise of flame instabilities [40]. With all the previously mentioned limitations, the chemical kinetics mechanisms [37, 45] and the formulated surrogates constitute a solid basis to provide a chemistry-grounded laminar flame speed estimation at engine-relevant conditions. In previous works, the authors identified a set of representative thermodynamic conditions, here called Engine Conditions (EC), experienced by a flame propagating from the burnt into the unburnt gases.

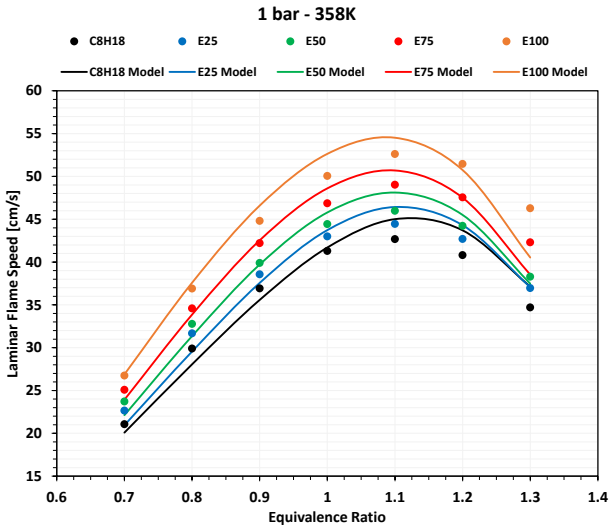

FIGURE 2. Experimental s_L values for different Isooctane/Ethanol blends from [40] and computed s_L values with the proposed methodology (solid lines).

These EC, represented by the red dots in Fig.3, were chosen in order to cover the possible thermodynamic states of the mixture, based on a wide dataset of SI engines characterized by different architectures, operating point and revving speeds [46, 47, 48, 49, 50, 51]. It is noteworthy that a $\pm 100\ K$ temperature interval was considered for the same pressure level, thus covering all the considered engine's pressure p and unburnt temperature T_u history. The aforementioned engine dataset is representative for gasoline powered units operated at full-load. It was specifically chosen to formulate correlations focusing on full-load conditions. Considering that several studies proved the increased cooling effect when SI engines are fueled with ethanol blended fuels [52, 53], it might be argued that blends with a high ethanol content might have an increased cooling effect compared to standard gasoline leading to p-T_u not covered by the chosen EC. Kasseris et al. [54] estimated in 35 K the increased cooling effect obtained when switching from standard gasoline fueling to E85. It can be concluded that the ensemble ECs are reasonably representative for the thermodynamic conditions expected in the case of blends characterized by extremely high ethanol content. Since the fuel model and the reference thermodynamic states were identified, chemical kinetics calculations were carried out with DARS v4.30 chemistry solver licensed by SIEMENS PLM. For each of the 33 ECs considered, 1D premixed freely propagating flame calculations were carried out for different equivalence ratio (Φ=0.4:0.1:2.0) and EGR mass fraction (Y_{EGR}=0:5:20) levels, in order to account for the mixture inhomogeneities arising with direct-injection fueling. As previously mentioned, two different chemical kinetics mechanisms are used to perform laminar flame speed calculations. This choice, as explained in previous studies [29, 30], was undertaken in order to reduce the uncertainties due to the usage of the mechanisms well beyond their validation range. Since two mechanisms are used for each single (p, T_u, Φ, EGR) condition, two different s_L solutions are computed from chemical kinetics calculations. Based on the previously explained rationale, the target s_L for the fitting procedure is defined as the algebraic mean of the s_L values obtained by the two datasets. Using this approach, a single s_L computed dataset is obtained, representing the algebraic mean of the calculated values with the two fuel models. A numerical methodology, extensively discussed by the authors in [29] and a modified version of the former in [30], is used to fit the calculated s_L dataset over the chosen ECs, identified by the red dots in Fig. 6. In the present study, the

latest version of the methodology [30], is used to derive the s_L correlations. Correlations are derived for E5, E20 and E85 fuels which are, or will feasibly be, the most widespread on the market. In fact, while E5 is now the standard reference blend for commercial gasolines [31], E85 is the leading blend powering flex-fuel vehicles (FFV) units [16]. On the other hand, E20 blend is expected to take over for E10 blend since the latter does not contain the required amount of Ethanol necessary to meet the ten percent bioenergy constraint imposed by the regulations coming into force in 2020 [3]. The key points of the methodologies are hereafter briefly summarized.

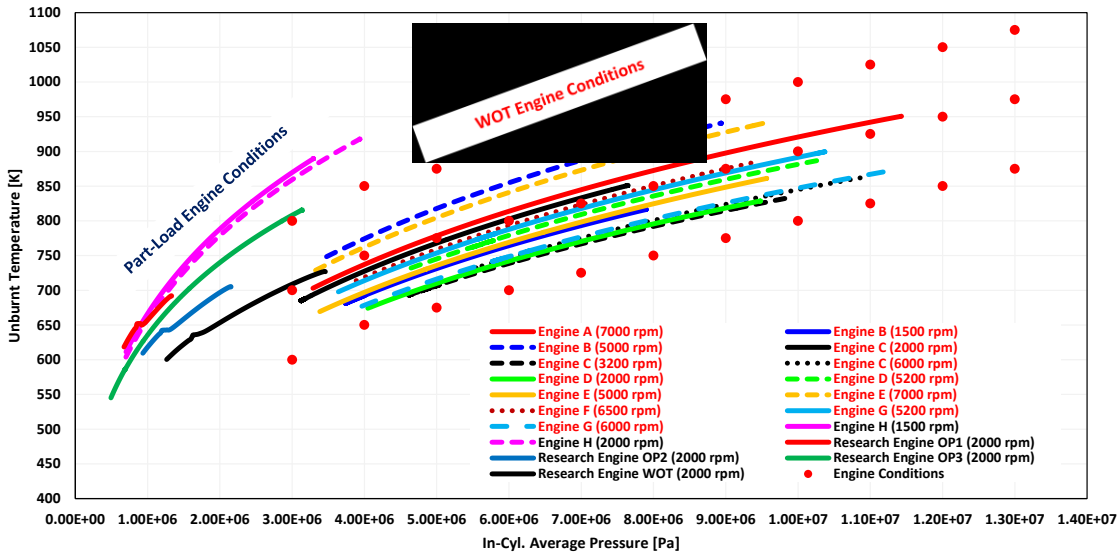

FIGURE 3. Pressure-Temperature history curves for a wide range of gasoline engines operated at full-load and part-load. Reference engine conditions used to perform chemistry-based s_L calculations are represented by red dots.

As in several other studies, a power-law relationship, in the form presented in Eq. 6, is used to model the dependence on pressure p, unburnt temperature T_u and equivalence ratio Φ once accurate forms for $s_{L,0}$, α and β are introduced. In order to properly fit the calculated s_L dataset, a fifth order logarithmic polynomial, as reported in Eq. 7, is used for each $s_{L,0}$, α and β.

$$s_L = s_{L,0}\left(\frac{T_u}{T_0}\right)^{\alpha}\left(\frac{p}{p_0}\right)^{\beta}(1 - f_{res}\cdot Y_{res}) \tag{6}$$

$$s_L = \left[\sum_{i=0}^{5} a_i \cdot log(\phi)^i\right]\cdot\left(\frac{T_u}{T_0}\right)^{\sum_{i=0}^{5} b_i\cdot log(\phi)^i}\cdot\left(\frac{p}{p_0}\right)^{\sum_{i=0}^{5} c_i\cdot log(\phi)^i} \tag{7}$$

The coefficients a_i, b_i, and c_i are used to fit the chemical kinetics calculations performed and are therefore used to introduce the equivalence ratio Φ, unburnt temperature T_u and pressure p dependence of s_L in the correlation, with respect to the selected reference condition ($T_0 = 825\,K$ and $p_0 = 15\,bar$). In order to find a closure to the s_L formulation presented in Eq. 7, six coefficients for a_i, b_i, and c_i (totaling eighteen coefficients) must be determined using a least square minimization approach. To obtain the final correlation for s_L, the dependence on the diluent mass fraction Y_{res} is introduced assuming a linear decreasing behavior; this is modelled by the f_{res} factor, which is calculated using the results obtained by the 1D simulations at different EGR levels. The outcome of the fitting procedure is the correlation presented in Eq. 8, which can be implemented in any CFD solver, provided the combustion model relies on the flamelet assumption.

$$s_{L,res} = \left[\sum_{i=0}^{5} a_i \cdot log(\phi)^i\right]\cdot\left(\frac{T_u}{T_0}\right)^{\sum_{i=0}^{5} b_i\cdot log(\phi)^i}\cdot\left(\frac{p}{p_0}\right)^{\sum_{i=0}^{5} c_i\cdot log(\phi)^i}\cdot(1 - f_{res}\cdot Y_{res}) \tag{8}$$

For the present study, a constant f_{res} value is used to model the average effect of the EGR level over different values of dilution rate. As previously stated, the laminar flame speed correlations in the present study will cover the entire range of equivalence ratio values typical of GDI applications ($0.4 \leq \Phi \leq 2.0$).The global s_L curves on the entire

equivalence ratio considered are finally presented in Fig. 4 for a selected number of ECs. For each EC, the s_L values calculated in the chemistry solver are reported as dots of different color and shape for the three different blends considered. The final outcome of the present study are the solid lines s_L values predicted by the correlations describing E5, E20 and E85 laminar flame speed on the set of engine conditions reported in Fig. 3.

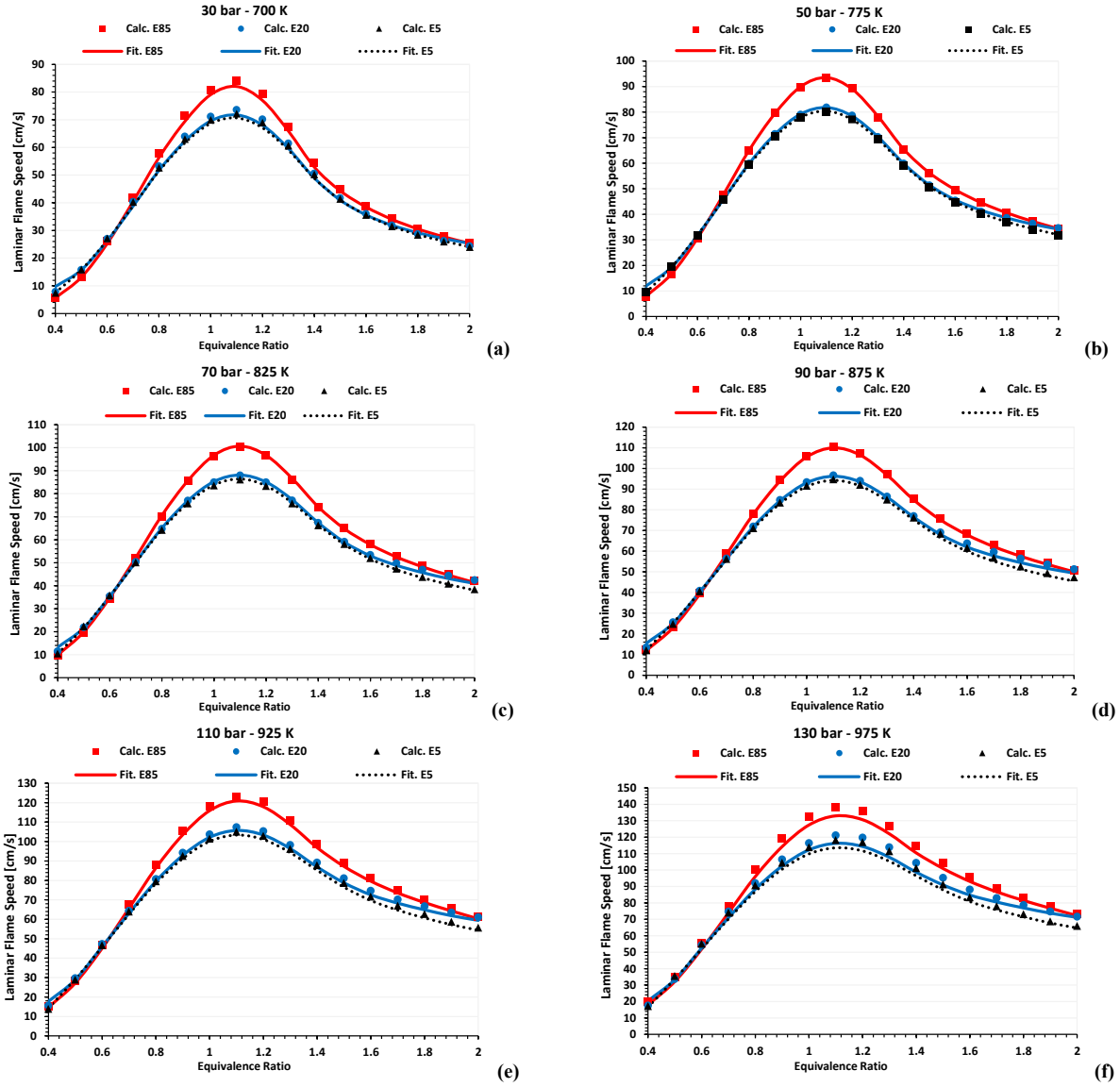

FIGURE 4. Laminar flame speed predicted by the proposed correlations for selected engine conditions. The s_L predicted by the E85 and E20 correlations are reported in solid red and blue lines, respectively. The s_L predicted by the E5 correlation is reported in dotted black line to improve the figures' readability. Target chemistry-based calculated data are reported with filled squares (E85), circles (E20) and triangles dots (E5).

As visible, the derived correlations are able to accurately describe the dependency of laminar flame speed on equivalence ratio, pressure and unburnt temperature predicted by the chemistry solver for the selected blends. As expected, the blends' s_L increases with an increasing ethanol content in the blend, especially in the rich mixtures where the abstraction of the oxygen atom in the ethanol molecule globally enhances the oxidation rate. Conversely, an increasing presence of ethanol has a detrimental effect on the flame propagation characteristics for very lean mixtures due to the increase amount of oxygen available. It is possible to conclude that the formulated fuel models are able to represent all the main effects expected by ethanol. The proposed s_L correlations, derived by the

polynomial fitting methodology previously described, are able to accurately describe both qualitatively and quantitatively the chemistry-grounded information derived by the 1D numerical simulations.

CONCLUSION

In the recent years, a general tightening of the emissions regulations worldwide led to an increasing interest in gasoline-ethanol fuel blends as a promising step towards more sustainable and cleaner power units. In the present study, dedicated ETRF fuel models were derived for E5, E20 and E85 gasoline ethanol blends. With the aim of providing a quantitative estimation of the propagating characteristics of the selected blends, 1D numerical simulations were carried out within a chemistry solver at full-load engine relevant conditions. A methodology previously introduced by the authors was used to generate laminar flame speed correlations for the three blends based on a polynomial fitting procedure. Such correlations can be implemented in any 3D-CFD flamelet combustion model to provide a quantitative estimation of E5, E20 and E85 laminar flame speed.

REFERENCES

1. *Official Journal of the European Union, L328, Volume 61, 21 December 2018, ISSN-1977-0677.*
2. *"Setting emission performance standards for new passenger cars and for new light commercial vehicles as part of the Union's integrated approach to reduce CO2 emissions from light-duty vehicles and amending Regulation (EC) No 715/2007", Regulation of the European parliament and of the council, COM (2017) 676 final, 2017/0293 (COD)*
3. *"Directive (EU) 2018/2001 of the European parliament and of the council of 11 December 2018 on the promotion of the use of energy from renewable sources", Official Journal of the European Union, L328/82, Volume 61, 21 December 2018, ISSN-1977-0677.*
4. *L.Tao et al. "Techno-economic analysis and life-cycle assessment of cellulosic isobutanol and comparison with cellulosic ethanol and n-butanol". Biofuels, Bioprod Biorefin 2014; 8(1):30-48. 10.1002/bbb.1431*
5. *L.G. Pereira et al"Economic and environmental assessment of n-butanol production in an integrated first and second generation sugarcane biorefinery: fermentative versus catalytic routes". Applied Energy 2015; 160:120-31. 10.1016/j.apenergy.2015.09.063.*
6. *A. Irimescu et al (2018). "Investigation on the effects of butanol and ethanol fueling on combustion and PM emissions in an optically accessible DISI engine". Fuel. (2018) 216. 121-141. 10.1016/j.fuel.2017.11.116.*
7. *J. Rawat et al. "Effect of Ethanol-Gasoline Blends on Corrosion Rate in the Presence of Different Materials of Construction used for Transportation, Storage and Fuel Tanks". SAE Technical Paper 2008-28-0125; 2008*
8. *P. Bielaczyc, et al. "An examination of the effect of ethanol–gasoline blends' physicochemical properties on emissions from a light-duty spark ignition engine". (2013) Fuel Processing Technology. 107. 50–63. 10.1016/j.fuproc.2012.07.030.*
9. *L. De Simio et al "Effect of Ethanol Content on Thermal Efficiency of a Spark-Ignition Light-Duty Engine". (2012) ISRN Renewable Energy. 2012. 10.5402/2012/219703.*
10. *A. F. Kheiralla et al. "Effect of Ethanol-Gasoline Blends on Fuel Properties Characteristics of Spark Ignition Engines. University of Khartoum Engineering Journal (UKEJ).Vol. 1, Issue 2:22-28. (2011)*
11. *M.A. Costagliola et al. "Performances and emissions of a 4-stroke motorcycle fuelled with ethanol/gasoline blends". Fuel. 183 (2016) 470-477. 10.1016/j.fuel.. 2016.06.105.*
12. *D. H. Qi, C. F. Lee (2014). "Combustion and emissions behaviour for ethanol–gasoline-blended fuels in a multipoint electronic fuel injection engine". International Journal of Sustainable Energy. 35. 1-16. (2014) 10.1080/14786451.2014.895004.*
13. *P. Sakthivel et al "Comparative studies on combustion, performance and emission characteristics of a two-wheeler with gasoline and 30% ethanol-gasoline blend using chassis dynamometer". Applied Thermal Engineering. (2018) 146. 10.1016/j.applthermaleng.2018.10.035.*
14. *P. Iodice et al. "Ethanol in gasoline fuel blends: Effect on fuel consumption and engine out emissions of SI engines in cold operating conditions". Applied Thermal Engineering. (2017) 130. 10.1016/j.applthermaleng.2017.11.090.*

15. *W. Hsieh et al. "Engine performance and pollutant emission of an SI engine using ethanol–gasoline blended fuels". Atmospheric Environment. 36. 403-410. (2002) 10.1016/S1352-2310(01)00508-8.*
16. *R. Suarez-Bertoa et al. "Impact of ethanol containing gasoline blends on emissions from a flex-fuel vehicle tested over the Worldwide Harmonized Light duty Test Cycle (WLTC)". Fuel. 143. (2014) 10.1016/j.fuel.2014.10.076.*
17. *F. Yüksel et al. "The use of ethanol–gasoline blend as a fuel in an SI engine". Renewable Energy. (2004) 29. 1181-1191. 10.1016/j.renene.2003.11.012.*
18. *T. Le Anh et al. (2011). "Investigation of motorcycle engine's characteristics fueled with ethanol-gasoline blends". The 4th AUN/SEED – Net Regional Conference on New and Renewable Energy (2011)*
19. *F. Liu et al. "An experimental study on soot distribution characteristics of ethanol-gasoline blends in laminar diffusion flames". Journal of the Energy Institute, Volume 91, Issue 6, 2018, Pages 997-1008, ISSN 1743-9671, https://doi.org/10.1016/j.joei.2017.07.008.*
20. *M. M. Maricq et al. "The impact of ethanol fuel blends on PM emissions from a light-duty GDI vehicle". Aerosol Sci. Tech. 46 (2012) 576-583*
21. *G. Karavalakis et al. "Evaluating the regulated emissions, air toxics, ultrafine particles, and black carbon from SI-PFI and SI-DI vehicles operating on different ethanol and iso-butanol blends". Fuel 218 (2014) 410-421*
22. *J. Cho et al. "Impact of intermediate ethanol blends on particulate matter emission from a spark ignition direct injection (SIDI) engine". Appl. Energy 160 (2015) 592-602*
23. *O. Colin et al. "The 3-Zone Extended Coherent Flame Model (ECFM-3Z) for computing premixed/diffusion combustion". (2004) Oil Gas Sci. Technol. – Rev. IFP 59, 6, 593-609*
24. *N. Peters. "Turbulent Combustion". Cambridge University Press, 2000*
25. *M. Metghalchi, J. C. Keck. "Burning velocities of mixtures of air with methanol, isooctane, and indolene at high pressure and temperature" Combustion and Flame, Vol. 48(1982), pp. 191-210.*
26. *Ö. Gülder. "Laminar Burning Velocities of Methanol, Ethanol, and Isooctane-Air Mixtures," Combustion Institute, 1982/pp. 275-281.*
27. *Ö. Gülder, "Correlations of Laminar Combustion Data for Alternative S.I. Engine Fuels," SAE Technical Paper 841000, 1984, https://doi.org/10.4271/841000*
28. *G. Broustail et al. "Experimental determination of laminar burning velocity for butanol and ethanol iso-octane blends". Fuel, Volume 90, Issue 1, 2011, Pages 1-6, ISSN 0016-2361, https://doi.org/10.1016/j.fuel.2010.09.021.*
29. *A. d'Adamo et al. "Chemistry-Based Laminar Flame Speed Correlations for a Wide Range of Engine Conditions for Iso-Octane, n-Heptane, Toluene and Gasoline Surrogate Fuels", SAE Technical Paper 2017-01-2190, 2017.*
30. *M. Del Pecchia et al. "Development of Chemistry-Based Laminar Flame Speed Correlation for Part-Load SI Conditions and Validation in a GDI Research Engine". (2018) SAE International Journal of Engines. 11. 10.4271/2018-01-0174, doi:10.4271/2018-01-0174.*
31. *C. Pera et al. "Methodology to define gasoline surrogates dedicated to auto-ignition in engines". Fuel, Volume 96, 2012, Pages 59-69, ISSN 0016-2361, https://doi.org/10.1016/j.fuel.2012.01.008.*
32. *Official Journal of the European Union, L140, Volume 52, 5 June 2009, ISSN-1725-2555.*
33. *B.M. Gauthier et al. "Shock tube determination of ignition delay times in full-blend and surrogate fuel mixtures". Combustion and Flame, Volume 139, Issue 4, 2004, Pages 300-311, ISSN 0010-2180, https://doi.org/10.1016/j.combustflame.2004.08.015.*
34. *J.C.G. Andrae et al. "Autoignition of toluene reference fuels at high pressures modeled with detailed chemical kinetics". Combustion and Flame, Volume 149, Issues 1–2, 2007, Pages 2-24, ISSN 0010-2180, https://doi.org/10.1016/j.combustflame.2006.12.014.*
35. *N. Morgan et al. "Mapping surrogate gasoline compositions into RON/MON space". Combustion and Flame, Volume 157, Issue 6, 2010, Pages 1122-1131, ISSN 0010-2180, https://doi.org/10.1016/j.combustflame.2010.02.003.*
36. *J.C.G. Andrae et al . "HCCI experiments with gasoline surrogate fuels modeled by a semidetailed chemical kinetic model", Combustion and Flame 156 (2009) 842-851.*
37. *J.C.G. Andrae, "Comprehensive chemical kinetic modeling of toluene reference fuels oxidation, Fuel, Volume 107, 2013, Pages 740-748, ISSN 0016-2361, https://doi.org/10.1016/j.fuel.2013.01.070.*
38. *P. Dirrenberger et al. Laminar burning velocity of gasolines with addition of ethanol. (2014) Fuel. 115. 162-169. 10.1016/j.fuel.2013.07.015.*

39. *S. Jerzembeck et al. "Laminar burning velocities at high pressure for primary reference fuels and gasoline: Experimental and numerical investigation", Combust and Flame 156 (2009) 292-301.*
40. *L. Sileghem et al. "Laminar burning velocity of gasoline and the gasoline surrogate components iso-octane, n-heptane and toluene". Fuel, Volume 112, 2013, Pages 355-365, ISSN 0016-2361, https://doi.org/10.1016/j.fuel.2013.05.049.*
41. *A. Ahmed et al. "A computational methodology for formulating gasoline surrogate fuels with accurate physical and chemical kinetic properties". Fuel, Volume 143, 2015, Pages 290-300, ISSN 0016-2361, https://doi.org/10.1016/j.fuel.2014.11.022.*
42. *L. Sileghem et al. (2012). "Alternative Fuels for Spark-Ignition Engines: Mixing Rules for the Laminar Burning Velocity of Gasoline–Alcohol Blends". (2012). Energy & Fuels. 26. 4721–4727. 10.1021/ef300393h.*
43. *V. Di Sarli et al. (2007). "Laminar burning velocity of hydrogen–methane/air premixed flames". (2007) International Journal of Hydrogen Energy. 32. 637-646. 10.1016/j.ijhydene.2006.05.016.*
44. *P. Ghosh et al. "Development of a detailed gasoline composition-based octane model". Ind Eng Chem Res 2006;45:337-45*
45. *E. Ranzi, A. Frassoldati, A. Stagni, M. Pelucchi et al. "Reduced Kinetic Schemes of Complex Reaction Systems: Fossil and Biomass-Derived Transportation Fuels". International Journal of Chemical Kinetics, doi:10.1002/kin.20867*
46. S. Fontanesi, *et al* "Integrated in-cylinder/CHT analysis for the prediction of abnormal combustion occurrence in gasoline engines". SAE Technical Papers, 2014. DOI: 10.4271/2014-01-1151
47. . S. Fontanesi *et al* "A methodology to improve knock tendency prediction in high performance engines". Energy Procedia, 45, pp. 769-778, 2014. DOI: 10.1016/j.egypro.2014.01.082
48. . G. Cantore *et al* "A methodology for in-cylinder flow field evaluation in a low stroke-to-bore SI engine". SAE Technical Papers, 2002. DOI: 10.4271/2002-01-1119
49. . F. Berni *et al* "A modified thermal wall function for the estimation of gas-to-wall heat fluxes in CFD in-cylinder simulations of high performance spark-ignition engines". Applied Thermal Engineering, 115, pp. 1045-1062, 2017. DOI: 10.1016/j.applthermaleng.2017.01.055
50. . S. Breda *et al.* "CFD analysis of combustion and knock in an optically accessible GDI engine". SAE International Journal of Engines, 9 (1), 2016.DOI: 10.4271/2016-01-0601
51. . S. Malaguti *et al* ."CFD investigation of wall wetting in a GDI engine under low temperature cranking operations". SAE Technical Papers, 2009. DOI: 10.4271/2009-01-0704
52. . G. da Silva *et al*. "The Effect of Charge Cooling on the RON of Ethanol/Gasoline Blends". (2013) SAE International Journal of Fuels and Lubricants. 6. 10.4271/2013-01-0886.
53. . Y. Huang *et al*. "Investigation to charge cooling effect and combustion characteristics of ethanol direct injection in a gasoline port injection engine". (2015). Applied Energy. 160. 244-254. 10.1016/j.apenergy.2015.09.059.
54. E. Kasseris *et al*. "Charge Cooling Effects on Knock Limits in SI DI Engines Using Gasoline/Ethanol Blends: Part 1-Quantifying Charge Cooling," SAE Technical Paper 2012-01-1275, 2012, https://doi.org/10.4271/2012-01-1275.

LAMINAR FLAME SPEED CORRELATION COEFFICIENTS

E85-Polynomial Fitting Coefficients				Pressure Scaling Lean-side Extension Fitting Coefficients		Pressure Scaling Rich-side Extension Fitting Coefficients	
	A	B	C				
1	1.009623E+02	2.718921E+00	-2.889658E-01	l3	6.068968E+00	r3	-1.045214E+00
2	8.114265E+01	-5.443706E-01	5.176360E-02	l2	9.544402E-01	r2	1.689523E+00
3	-3.307984E+02	6.180692E+00	-4.658047E-01	l1	-3.489660E+00	r1	-1.338939E+00
4	-7.158979E+02	1.010163E+01	5.374411E-01	l0	1.000000E+00	r0	9.942390E-01
5	4.189288E+02	-1.435391E+01	4.848613E+00	m2	4.682530E-01	m1	2.301505E-01
6	2.422162E+03	-6.368069E+01	6.666948E+00				
Stoich. Air-Fuel ratio			9.755				
Kegr			2.07				
p0_fit			8.00E+06				
T0_fit			850.00				

Temperature Scaling Rich-side Extension Fitting Coefficients						
	m LOW (rml)	q LOW (rql)	m MED (rmm)	q MED (rqm)	m HIGH (rmh)	q HIGH (rqh)
4	-2.894646E+00	4.433458E+00	-1.808167E+00	3.088075E+00	3.592250E+00	-5.462787E+00
3	2.147954E+01	-3.324583E+01	1.341226E+01	-2.349130E+01	-2.497154E+01	3.700372E+01
2	-6.031420E+01	9.452988E+01	-3.812400E+01	6.844413E+01	6.346575E+01	-9.076880E+01
1	7.614266E+01	-1.214530E+02	4.933375E+01	-9.100407E+01	-6.908535E+01	9.333645E+01
0	-3.618666E+01	5.992599E+01	-2.415342E+01	4.677931E+01	2.712505E+01	-3.244142E+01
Temperature Scaling Lean-side Extension Fitting Coefficients						
	m LOW (lml)	q LOW (lql)	m MED (lmm)	q MED (lqm)	m HIGH (lmh)	q HIGH (lqh)
2	-6.285140E+00	1.347990E+01	-4.378305E+00	1.091458E+01	-4.950865E+00	1.123173E+01
1	6.186889E+00	-1.101462E+01	4.003308E+00	-8.026481E+00	3.779165E+00	-7.125334E+00
0	-1.241555E+00	2.123534E+00	-6.803398E-01	1.345030E+00	-2.994363E-01	6.477671E-01
Temperature- Pressure Scaling Coefficients						
Pressure weight			1.00			
Temperature weight			5.00			
Total weight			6.00			
pref_fit			8.00E+06			
Tref_fit			600.00			